Precession Caused by Gravitational Waves

Ali Seraj
Centre for Gravitational Waves, Université Libre de Bruxelles and International Solvay Institutes, CP 231, B-1050 Brussels, Belgium

Blagoje Oblak
CPHT, CNRS, Ecole Polytechnique, IP Paris, F-91128 Palaiseau, France and LPTHE, CNRS, Sorbonne Université, 75252 Paris Cedex 05, France

(Received 25 March 2022; accepted 11 July 2022; published 2 August 2022)

We show that gravitational waves cause freely falling gyroscopes to precess relative to fixed distant stars, extending the stationary Lense-Thirring effect. The precession rate decays as the square of the inverse distance to the source and is proportional to a suitable Noether current for dual asymptotic symmetries at null infinity. Integrating the rate over time yields a net rotation—a "gyroscopic memory"—whose angle reproduces the known spin memory effect but also contains an extra contribution due to the generator of gravitational electric-magnetic duality. The angle's order of magnitude for the first Laser Interferometer Gravitational Wave Observatory signal is estimated to be $\Phi \sim 10^{-35}$ arc sec near Earth, but the effect may be substantially larger for supermassive black hole mergers.

DOI: 10.1103/PhysRevLett.129.061101

Introduction.—Consider an observer floating freely in outer space, carrying a spinning gyroscope. The observer looks at fixed distant stars in order to measure the gyroscope's orientation. When a localized source emits a burst of gravitational waves that crosses the observer's path, the gyroscope precesses and eventually settles in a new orientation (Fig. 1); the corresponding rotation angle carries a "memory" of the wave profile. The goal of this Letter is to describe this precession and the ensuing memory effect.

The motivation for this investigation is twofold. The first is the recent breakthrough observation of gravitational waves [1], which makes it realistic to seek their measurable signatures. In particular, "memory effects" [2–12] sensitive to the net offset of metric components after a gravitational wave burst (see Fig. 2) may be observable in the near future [13–15]. The second motivation has to do with fundamental symmetries of classical and quantum gravity. Indeed, asymptotically Minkowskian space-time metrics enjoy an infinite-dimensional "Bondi-Metzner-Sachs symmetry" [16–19], whose Noether currents at null infinity were recently related to the displacement memory that affects nearby freely falling test masses [20]. In a similar vein, the rate of gyroscopic precession found here turns out to coincide with a current [21,22] for so-called dual supertranslations [23–30]. Furthermore, the net change of orientation before and after the passage of waves involves a superrotation charge [31–33] and a generator of local gravitational electric-magnetic duality transformations. To our knowledge, this is the first appearance of such dual symmetries in a simple local measurement protocol for gravitational waves.

There is, in fact, a third, perhaps more academic, motivation for this Letter. Indeed, while our results are related to deep properties of the gravitational phase space at the forefront of research, our method is comparatively elementary: it consists of rewriting the parallel transport equation of a spin vector in a radiative space-time, with respect to a tetrad whose elements point toward fixed distant stars. The computation is thus an exercise that generalizes Lense-Thirring precession ([34] Sec. 40.7) to radiative metrics, and it could have been carried out 60 years ago [16,17]. It seems important indeed to fill such a gap in the literature.

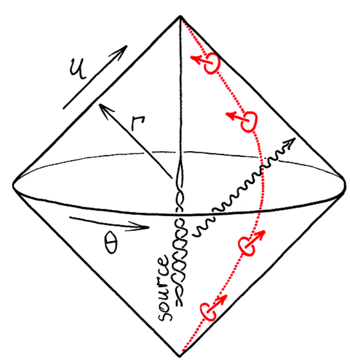

FIG. 1. The world line of a freely falling observer with a gyroscope, represented here (in red) in a Penrose diagram of near-Minkowski space. The gyroscope's spin is parallel transported along its trajectory, but the passage of gravitational waves causes its orientation to change relative to fixed distant stars. Bondi coordinates (u, r, θ^a) are included; the source of radiation is located at the origin $r = 0$.

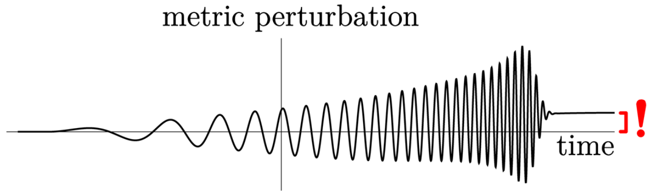

FIG. 2. A cartoon of the typical local metric perturbation caused by gravitational waves. Even after the end of the disturbance, some metric components [typically some function of the shear C_{ab} in Eq. (1)] differ from their initial value by an amount that depends on the waveform. This net offset has potentially observable consequences; one of them is the gyroscopic memory described here. See the last subsection for a more detailed discussion of this plot in the gyroscopic context.

The Letter is organized as follows. The second section sets the stage by displaying the (Bondi) coordinates and metric [16,17] to be used throughout and contains a description of the tetrad with respect to which precession is to be evaluated. The third section is then devoted to our results, namely, the expression of the precession rate in terms of a "dual covariant mass aspect" [21,22] and that of orientation memory in terms of a surface charge, its flux, and a generator of electric-magnetic duality. Aside from the latter, this actually reproduces the spin memory effect [11] as a special case. Note that computational details are omitted throughout: they are relegated to the longer companion paper [35].

Metric and tetrad.—This section introduces Bondi coordinates, the corresponding asymptotically flat metrics, and the tetrad that will be used in the next section to measure the gyroscope's orientation relative to fixed distant stars. Readers familiar with the Bondi metric ansatz may jump straight to the discussion of the tetrad below Eq. (3).

First choose an origin in space and label the points of the four-dimensional space-time manifold by retarded Bondi coordinates: an areal distance r, a retarded time u, and angular coordinates θ^a ($a = 1, 2$) on a unit celestial sphere with metric $q_{ab}(\theta) d\theta^a d\theta^b$ (see Fig. 1). Any outgoing lightlike ray then propagates so as to eventually reach future null infinity, i.e., the region $r \to \infty$ with finite u. Accordingly, we assume throughout that our observer is located at large r. It is then meaningful to expand the components of the space-time metric as asymptotic series in $1/r$ [36],

$$
\begin{aligned}
ds^2 \sim & -\left(1-\frac{2m}{r}-\frac{2F}{r^2}\right)du^2 - 2\left(1-\frac{C^2}{16r^2}\right)du\,dr \\
& + \left(r^2 q_{ab} + r C_{ab} + \frac{1}{4} q_{ab} C^2\right) d\theta^a d\theta^b \\
& + 2\left\{\frac{1}{2}D^b C_{ab} + \frac{1}{r}\left[\frac{2}{3}L_a - \frac{1}{16}\partial_a(C^2)\right]\right\} du\, d\theta^a, \quad (1)
\end{aligned}
$$

where the functions m, F, C_{ab}, and L_a only depend on (u, θ). (We also write $C^2 \equiv C_{ab}C^{ab}$ to reduce clutter, with indices raised and lowered thanks to the metric q_{ab}; D_a is the covariant derivative on S^2.) The radial dependence is thus explicit and the metric reduces to the pure Minkowski form $ds^2 = -du^2 - 2du\,dr + r^2 q_{ab} d\theta^a d\theta^b$ in the limit $r \to \infty$.

The most important quantity in (1) is the (symmetric and traceless) asymptotic shear tensor $C_{ab}(u, \theta)$, which contains all the information about radiation. Its time dependence is unconstrained and determines the news tensor $N_{ab} \equiv \partial_u C_{ab}$ that will play a key role below. The function $m(u, \theta)$ is the Bondi mass aspect and $L_a(u, \theta)$ is the angular momentum aspect, respectively, measuring densities of energy and angular momentum at null infinity. Their time dependence is fixed by the shear and news tensors through so-called balance equations [36],

$$\dot{m} = \frac{1}{4} D_a D_b N^{ab} - \frac{1}{8} N_{ab} N^{ab}, \quad (2a)$$

$$\dot{L}_a = D_a m + \frac{1}{2} D^b D_{[a} D^c C_{b]c} - \mathcal{J}_a, \quad (2b)$$

where $\dot{X} \equiv \partial_u X$, while $\mathcal{J}$ is a local quadratic flux,

$$\mathcal{J}_a \equiv -\frac{1}{4} D_b (N^{bc} C_{ac}) - \frac{1}{2} D_b N^{bc} C_{ac}, \quad (3)$$

which will eventually turn out to affect orientation memory. The remaining function F in (1) is then given by $F = -(1/32)C^2 - (1/6)(D_a L^a) - (1/8)(DC)^2$, where we let $(DC)^2 \equiv D_b C^{ab} D^c C_{ac}$ for brevity.

The full metric (1) contains numerous subleading corrections in $1/r$, all of which we omit since they will play no role below. Crucially, all subleading terms are determined by leading metric data up to time-independent "integration functions" on celestial spheres [19,37]. This is similar to mass and angular momentum, whose time evolution (2) is entirely fixed by news so that only the initial conditions $m(u_0, \theta)$ and $L_a(u_0, \theta)$ are arbitrary.

Now consider a freely falling observer at large r in an asymptotically flat metric (1). We wish to build an orthonormal tetrad $\{\boldsymbol{f}_{\hat{\mu}} | \mu = 0, 1, 2, 3\}$ such that $\boldsymbol{f}_{\hat{0}} = \boldsymbol{u}$ is the observer's proper velocity, while $\boldsymbol{f}_{\hat{\imath}}$ ($i = 1, 2, 3$) are spacelike vectors pointing toward fixed distant stars at infinity. (Hatted indices label tetrad elements, and they are raised or lowered using the inertial Minkowski metric.) In practice, Bondi coordinates heavily rely on a choice of origin—the location of the source of radiation. Accordingly, we first build a "source-oriented" tetrad $\{\boldsymbol{e}_{\hat{\mu}}\}$, then perform angle-dependent rotations so as to produce the desired frame $\{\boldsymbol{f}_{\hat{\mu}}\}$, which we call "star-oriented."

Our starting point is the observer's proper velocity

$$\boldsymbol{e}_{\hat{0}} = \boldsymbol{f}_{\hat{0}} = \boldsymbol{u} = \gamma(\partial_u + v^r\partial_r + v^a\partial_a), \tag{4}$$

i.e., the zeroth element of both tetrads. In these terms, solving the geodesic equation for the metric (1) with the condition $\boldsymbol{u} \sim \partial_u$ at large r (the observer is asymptotically at rest) yields

$$\gamma = 1 + \frac{m_0}{r} + \frac{\gamma_2}{r^2}, \qquad \gamma_2 \equiv \frac{1}{16}C^2 + \int m, \tag{5a}$$

$$v^r = \frac{m - m_0}{r} + \frac{1}{r^2}\left[-\gamma_2 - \frac{1}{6}D_a L^a - \frac{1}{8}(DC)^2\right], \tag{5b}$$

$$v^a = -\frac{1}{2r^2}D_b C^{ab} + \frac{1}{r^3}\left(D^a\gamma_2 - \frac{2}{3}L^a + \frac{1}{2}C^{ab}D^c C_{bc}\right), \tag{5c}$$

with $m_0 \equiv m(u_0, \theta)$ as the initial Bondi mass aspect and $\int m \equiv \int_{u_0}^{u} du' m$. Only spatial tetrad elements thus remain to be found. In the source-oriented case, one first obtains the radial vector $\boldsymbol{e}_{\hat{r}}$ by following an outgoing null radial geodesic, projecting out the $\boldsymbol{u}$ component of its velocity and finally expanding in $1/r$, which yields $\boldsymbol{e}_{\hat{r}} \sim (1/\gamma)[1 + (1/r^2)C^2/16]\partial_r - \boldsymbol{u}$. The tetrad is then completed by picking an orthonormal dyad $\zeta_{\hat{a}}$ on the unit sphere and expanding angular tetrad elements as

$$\boldsymbol{e}_{\hat{a}} \sim \frac{1}{r}\zeta_{\hat{a}}{}^{b}\left(\delta^a_b - \frac{1}{2r}C^a_b + \frac{1}{16r^2}C^2\delta^a_b\right)\left(\partial_a + \frac{1}{r}D_a\int m\partial_r\right). \tag{6}$$

This furnishes an explicit source-oriented Lorentz frame $\{\boldsymbol{e}_{\hat{0}}, \boldsymbol{e}_{\hat{r}}, \boldsymbol{e}_{\hat{a}}\}$, written here perturbatively in $1/r$.

Obtaining a tetrad whose spatial vectors point toward fixed distant stars requires an extra step (see Fig. 3), as the

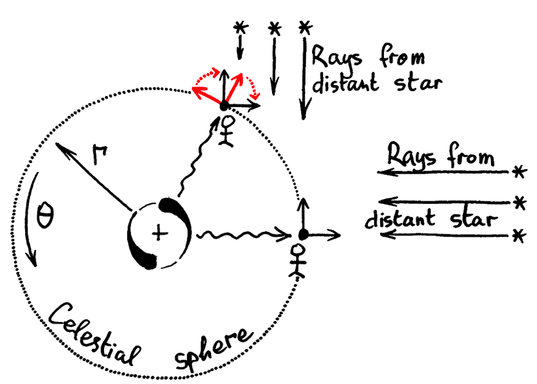

FIG. 3. In Bondi coordinates, the most natural tetrad $\{\boldsymbol{e}_{\hat{\mu}}\}$ is a source-oriented one (with a radial vector $\boldsymbol{e}_{\hat{r}}$ aligned with outgoing null geodesics). Converting such a frame into a tetrad $\{\boldsymbol{f}_{\hat{\mu}}\}$ pointing toward fixed distant stars requires a local rotation $R(\theta)$, as in Eq. (7).

spatial vectors $\{\boldsymbol{e}_{\hat{r}}, \boldsymbol{e}_{\hat{a}}\}$ need to be rotated in an angle-dependent manner. This is intuitively obvious: even in pure Minkowski space, the source-oriented tetrad of a freely falling observer must rotate continuously so that its vector $\boldsymbol{e}_{\hat{r}}$ points toward the origin. Any gyroscope with non-zero angular velocity trivially precesses relative to this tetrad, even without radiation. One may therefore compensate this effect by defining transformed tetrad vectors

$$\boldsymbol{f}_{\hat{i}} = R_{\hat{i}}{}^{\hat{j}}(\theta)\boldsymbol{e}_{\hat{j}}, \tag{7}$$

where the local rotation matrix is a path-ordered exponential $R(\theta) = P\exp\int_{\theta_0}^{\theta}\bar{\omega}$ of the spin connection $\bar{\omega}$ of the flat space triad $\{\partial_r - \partial_u, (1/r)\zeta_{\hat{a}}\}$, with $\zeta_{\hat{a}}$ the spherical dyad introduced above (6). Explicitly, this background spin connection has components $\bar{\omega}_{\hat{a}\hat{r}} = \zeta_{\hat{a}a}d\theta^a$ and $\bar{\omega}_{\hat{a}\hat{b}} = \zeta_{\hat{a}}{}^{a}D_b\zeta_{\hat{b}a}d\theta^b$. The observer thus uses flatness at infinity to adjust their frame by a rotation that is purely determined by fixed asymptotic structures $(q_{ab}, \zeta_{\hat{a}}{}^{b})$, regardless of the presence of bulk radiation.

The choice of path defining $R(\theta)$ generally affects its value, but it is ultimately irrelevant: for our purposes, it suffices that $R(\theta_0) = \mathbb{I}$ be the identity at the observer's initial angular position θ_0, i.e., that the source- and star-oriented tetrads initially coincide. As a result, the only relevant contribution of $R(\theta)$ to the transformation law of the spin connection $\omega \to R\omega R^{-1} + RdR^{-1}$ stems from the inhomogeneous term, which cancels as desired the uninteresting rotation due to the observer's motion on a celestial sphere. A star-oriented tetrad has thus been defined, and one may finally use it to measure the precession of gyroscopes.

Precession and memory.—This section presents our results: a formula for the gyroscopic precession rate in terms of shear and news tensors and the resulting expression for net orientation memory [see Eqs. (11) and (15) below]. We use the star-oriented frame $\boldsymbol{f}_{\hat{\mu}}$ and focus on freely falling observers (accelerated observers are addressed in [35]).

Any small freely falling gyroscope has a spin vector $\boldsymbol{S}$ that is parallel transported along its world line: $\nabla_{\boldsymbol{u}}\boldsymbol{S} = 0$ in terms of proper velocity $\boldsymbol{u}$. Now let $\{\boldsymbol{f}_{\hat{\mu}}\}$ be a tetrad at the gyroscope's location such that $\boldsymbol{f}_{\hat{0}} = \boldsymbol{u}$. Then the spin vector may be written as $\boldsymbol{S} = S^{\hat{i}}\boldsymbol{f}_{\hat{i}}$ and parallel transport becomes equivalent to a precession equation

$$\frac{dS^{\hat{i}}(\tau)}{d\tau} = \Omega^{\hat{i}}_{\hat{j}}(\tau)S^{\hat{j}}(\tau), \tag{8}$$

where τ is the observer's proper time and the angular velocity (precession rate) matrix $\Omega^{\hat{i}}_{\hat{j}}(\tau)$ is the projection along $\boldsymbol{u}$ of the spin connection ω of the tetrad $\{\boldsymbol{f}_{\hat{\mu}}\}$,

$$\Omega^{\hat{i}\hat{j}} = -u^\alpha \omega_\alpha{}^{\hat{i}\hat{j}}, \qquad \omega_\mu{}^{\hat{\mu}\hat{\nu}} \equiv f^{\hat{\mu}}{}_\alpha \nabla_\mu f^{\hat{\nu}\alpha}. \tag{9}$$

The gyroscope's precession rate is thus wholly determined by the spin connection evaluated along the observer's trajectory. In practice, it is simpler to compute the spin connection of the source-oriented tetrad $\{\boldsymbol{e}_{\hat{\mu}}\}$ defined in Eqs. (4)–(6), then use the rotation (7) to obtain the spin connection of $\boldsymbol{f}_{\hat{\mu}}$. At leading order in $1/r$ along the world line of the observer, this yields

$$\omega_{\hat{r}\hat{a}} \sim \zeta_{\hat{a}}{}^a \left(\frac{1}{4r^2} N_{ab} D_c C^{bc} du + \frac{D^b C_{ab}}{2r^2} dr + \frac{N_{ab}}{2} d\theta^b \right), \tag{10a}$$

$$\omega_{\hat{a}\hat{b}} \sim -\frac{1}{2r^2} \zeta_{\hat{a}}{}^a \zeta_{\hat{b}}{}^b \left(D_{[a} D^c C_{b]c} - \frac{1}{2} N_{c[a} C^c{}_{b]} \right) du + \mathcal{O}(r^{-3}) dr + \mathcal{O}(r^{-1}) d\theta^a, \tag{10b}$$

where $A_{[a}B_{b]} \equiv \frac{1}{2}(A_a B_b - A_b B_a)$. Note that this only depends on the shear C_{ab} and the news N_{ab}, without any influence of mass or angular momentum aspects: the latter only appear in subleading terms that are neglected here. [This notably includes Lense-Thirring precession ([34] Sec. 40.7) at order $\mathcal{O}(r^{-3})$.]

It is straightforward to obtain the angular velocity matrix (9) from the geodesic velocity (4) and the spin connection (10). Indeed, one finds $\Omega_{\hat{a}\hat{r}} = \mathcal{O}(r^{-3})$ and

$$\Omega_{\hat{a}\hat{b}} \sim \frac{\epsilon_{\hat{a}\hat{b}}}{r^2} \widetilde{\mathcal{M}}, \quad \widetilde{\mathcal{M}} \equiv \frac{1}{4} D_a D_b \tilde{C}^{ab} - \frac{1}{8} N_{ab} \tilde{C}^{ab}, \tag{11}$$

where the "dual shear tensor" is $\tilde{C}_{ab} \equiv \epsilon_{ca} C_b{}^c$ in terms of the Levi-Civita tensor density on the unit S^2. This is our first main conclusion: the precession of a gyroscope occurs, at leading order, in the plane $\hat{a}\,\hat{b}$ orthogonal to incoming radiation. Furthermore, the precession rate is proportional to a celestially local current $\widetilde{\mathcal{M}}(u,\theta)$, namely, the dual covariant mass aspect [21,22] closely related to the symmetry of asymptotically flat gravity under so-called dual supertranslations [23–30]. As announced in the Introduction, we have thus found that the precession caused by gravitational waves probes a fundamental property of the gravitational phase space. This point will be further supported in the last subsection by a relation between orientation memory and the generator of gravitational electric-magnetic duality.

For future reference, it is useful to write tensors on celestial spheres in terms of (pseudo)scalar functions with definite parity. Let, therefore, angular momentum and shear be written as

$$L_a \equiv D_a L^+ + \epsilon_{ab} D^b L^-, \tag{12a}$$

$$C_{ab} \equiv D_{(a} D_{b)} C^+ - \frac{1}{2} q_{ab} D^2 C^+ + \epsilon_{c(a} D_{b)} D^c C^-, \tag{12b}$$

where $A_{(a}B_{b)} \equiv \frac{1}{2}(A_a B_b + A_b B_a)$ and the superscript $+$ (respectively, $-$) denotes even (respectively, odd) functions. The term linear in C in (11) can then be recast as $\frac{1}{8} D^2 (D^2 + 2) C^-$, which is manifestly odd. Furthermore, the balance equation (2b) allows us to relate this term to the time derivative of the odd component of angular momentum and its flux as

$$\widetilde{\mathcal{M}} = \dot{L}^- + \mathcal{J}^- - \frac{1}{8} N_{ab} \tilde{C}^{ab}, \tag{13}$$

where $\mathcal{J}^- = D^{-2}(\epsilon^{ab} D_b \mathcal{J}_a)$ and D^{-2} is the inverse of the Laplacian on S^2, involving Green's function G such that $D^2 G(\theta, \theta') = (1/\sqrt{q}) \delta(\theta - \theta') - (1/4\pi)$. This confirms the expected absence of precession in nonradiative space-times, since $N_{ab} = 0$ also implies $\dot{L}^- = \mathcal{J}^- = 0$ (at least in the absence of Newman-Unti-Tamburino charges [30]). Relative to fixed distant stars, precession thus occurs only during the passage of a wave. It is therefore meaningful to compute the net change of orientation due to a burst of radiation.

Indeed, one can readily write the solution of the precession equation (8) as a time-ordered exponential of the matrix Ω acting on some initial spin $\boldsymbol{S}_{\text{init}}$. In practice, only the first nontrivial term of this expansion is reliable, since the angular velocity (11) is of order $\mathcal{O}(1/r^2)$ anyway and higher-order terms of the exponential series are affected by subleading $1/r$ corrections that have been neglected here. Accordingly, the leading-order change of orientation of the gyroscope's axis is given by $\Delta S^{\hat{r}} = \mathcal{O}(r^{-3})$ and $\Delta S^{\hat{a}} = \Phi \epsilon^{\hat{a}\hat{b}} S^{\hat{b}}_{\text{init}} + \mathcal{O}(r^{-3})$, where the rotation angle in the $\hat{a}\,\hat{b}$ plane is obtained by integrating the covariant dual mass aspect (13) over time,

$$\Phi = \int du \frac{\widetilde{\mathcal{M}}}{r^2} = \frac{1}{r^2} \left[\Delta L^- + \int du \left(\mathcal{J}^- - \frac{1}{8} N_{ab} \tilde{C}^{ab} \right) \right]. \tag{14}$$

The fact that $\Phi \neq 0$ is the aforementioned memory effect: the passage of waves entails a permanent change of orientation, sensitive to a specific combination $\widetilde{\mathcal{M}}$ of metric components. The latter can be rewritten more suggestively by "inverting" the parity decomposition (12) under the assumption (without loss of generality) that $L^\pm$ have vanishing average on S^2, while $C^\pm$ both have vanishing harmonics of order $\ell = 0, 1$. This rephrases the memory effect (14) as

$$\Phi = \frac{8\pi}{r^2} \left(\Delta Q_Y + \mathcal{F}_Y - \frac{1}{64\pi} \int du\, N_{ab} \tilde{C}^{ab} \right), \tag{15}$$

where all terms on the right-hand side are evaluated at θ and we have introduced a divergence-free vector field

$Y^a(\theta') \equiv \epsilon^{ab} D_b G(\theta, \theta')$, while $Q_Y \equiv (1/8\pi) \oint \sqrt{q} d^2\theta' Y^a L_a$ is the associated superangular momentum charge [33] and $\mathcal{F}_Y \equiv (1/8\pi) \oint \sqrt{q} d^2\theta' Y^a \mathcal{J}_a$ is its flux. This makes it manifest that the first two terms of gyroscopic memory (namely, $\Delta Q + \mathcal{F}$) reproduce the spin memory effect [11]. Crucially, however, Eq. (15) involves an additional nonlinear term $\propto \int N_{ab} \tilde{C}^{ab}$; the latter is nothing but the Hamiltonian generator of local electric-magnetic duality transformations on radiative phase space endowed with its standard symplectic form [38]. This exhibits once more the deep relation between gyroscopic memory and crucial gravitational symmetries.

The nonvanishing value of (15) also illustrates the general memory mechanism suggested in Fig. 2. In the context of displacement memory [20], the "metric perturbation" of Fig. 2 is the shear C_{ab} and the net change ΔC_{ab} measures the angular deviation of nearby geodesics. Gyroscopic memory is more subtle in that respect, as the perturbation should now be seen as a time integral of dual shear through the dual covariant mass aspect of Eq. (11). The presence of such time-integrated metric perturbations is typical of subleading memory effects [39–41].

To conclude, let us estimate the magnitude of the memory effect (15): it falls off as $1/r^2$ and is in this sense dominant with respect to Lense-Thirring precession, which falls off as $1/r^3$. Could it then be possible to observe the precession described here? The answer is unclear at the moment, as realistic values of (15) are tiny. Indeed, elementary dimensional analysis suggests that the order of magnitude of (15) for a bound binary system with mass scale M is

$$\Phi \sim \frac{G^2}{c^4} \frac{M^2}{r^2} \simeq 2 \times 10^{-39} \left(\frac{M/M_\odot}{r/1 \text{ Mpc}} \right)^2, \qquad (16)$$

where G is Newton's constant, c is the speed of light in vacuum, and $M_\odot$ is the solar mass. This is manifestly exceedingly weak for the common values of mass and distance ($M \simeq 30\ M_\odot$ and $r \simeq 400$ Mpc for the seminal LIGO Collaboration observation [1]). It is nevertheless conceivable that the effect will some day be observable in extreme events, such as supermassive black hole mergers, for which values on the order of $\Phi \simeq 10^{-26}$ rad are not far-fetched. Also note that the effect is independent of the gyroscope's spin and inertia, so one may even resort to distant pulsars (whose high mass and low volume reduce nongravitational environmental effects) as radiation probes. Small rotations of a pulsar's axis could then conceivably be measured: for instance, a $\Phi \sim 10^{-26}$ rad change in the angle of an idealized narrow beam emitted 10^3 light years away from the Solar System modifies the position of the resulting light spot on Earth by about 10^{-7} m. We hope to further develop some of these ideas in future work: it would be fascinating indeed to observe gravitational memory effects with the simple gyroscopic setup described here.

We are grateful to Glenn Barnich, François Mernier, and Roberto Oliveri for insightful comments on an early draft of this Letter and to Miguel Paulos for suggesting to use pulsars as gyroscopes. The work of A. S. is funded by the European Union's Horizon 2020 research and innovation program under the Marie Skłodowska-Curie Grant Agreement No. 801505. The work of B. O. is supported by the ANR grant *TopO* No. ANR-17-CE30-0013-01 and by the European Union's Horizon 2020 research and innovation program under the Marie Skłodowska-Curie Grant Agreement No. 846244.

[1] B. P. Abbott *et al.* (LIGO Scientific and Virgo Collaborations), Observation of Gravitational Waves from a Binary Black Hole Merger, Phys. Rev. Lett. **116**, 061102 (2016).

[2] Y. B. Zel'dovich and A. G. Polnarev, Radiation of gravitational waves by a cluster of superdense stars, Sov. Astron. **18**, 17 (1974).

[3] V. B. Braginsky and L. P. Grishchuk, Kinematic resonance and memory effect in free mass gravitational antennas, Sov. Phys. JETP **62**, 427 (1985).

[4] V. B. Braginsky and K. S. Thorne, Gravitational-wave bursts with memory and experimental prospects, Nature (London) **327**, 123 (1987).

[5] D. Christodoulou, Nonlinear Nature of Gravitation and Gravitational Wave Experiments, Phys. Rev. Lett. **67**, 1486 (1991).

[6] L. Blanchet and T. Damour, Hereditary effects in gravitational radiation, Phys. Rev. D **46**, 4304 (1992).

[7] P. M. Zhang, C. Duval, G. W. Gibbons, and P. A. Horvathy, The memory effect for plane gravitational waves, Phys. Lett. B **772**, 743 (2017).

[8] P. M. Zhang, C. Duval, G. W. Gibbons, and P. A. Horvathy, Soft gravitons and the memory effect for plane gravitational waves, Phys. Rev. D **96**, 064013 (2017).

[9] E. E. Flanagan, A. M. Grant, A. I. Harte, and D. A. Nichols, Persistent gravitational wave observables: General framework, Phys. Rev. D **99**, 084044 (2019).

[10] A. K. Divakarla and B. F. Whiting, First-order velocity memory effect from compact binary coalescing sources, Phys. Rev. D **104**, 064001 (2021).

[11] S. Pasterski, A. Strominger, and A. Zhiboedov, New gravitational memories, J. High Energy Phys. 12 (2016) 053.

[12] P. Mao and X. Wu, More on gravitational memory, J. High Energy Phys. 05 (2019) 058.

[13] M. Favata, The gravitational-wave memory effect, Classical Quantum Gravity **27**, 084036 (2010).

[14] P. D. Lasky, E. Thrane, Y. Levin, J. Blackman, and Y. Chen, Detecting Gravitational-Wave Memory with LIGO: Implications of GW150914, Phys. Rev. Lett. **117**, 061102 (2016).

[15] O. M. Boersma, D. A. Nichols, and P. Schmidt, Forecasts for detecting the gravitational-wave memory effect with Advanced LIGO and Virgo, Phys. Rev. D **101**, 083026 (2020).

[16] H. Bondi, M. G. J. van der Burg, and A. W. K. Metzner, Gravitational waves in general relativity. 7. Waves from axisymmetric isolated systems, Proc. R. Soc. A **269**, 21 (1962).
[17] R. Sachs, Asymptotic symmetries in gravitational theory, Phys. Rev. **128**, 2851 (1962).
[18] G. Barnich and C. Troessaert, Symmetries of Asymptotically Flat 4 Dimensional Spacetimes at Null Infinity Revisited, Phys. Rev. Lett. **105**, 111103 (2010).
[19] G. Barnich and C. Troessaert, Aspects of the BMS/CFT correspondence, J. High Energy Phys. 05 (2010) 062.
[20] A. Strominger and A. Zhiboedov, Gravitational memory, BMS supertranslations and soft theorems, J. High Energy Phys. 01 (2016) 086.
[21] L. Freidel, R. Oliveri, D. Pranzetti, and S. Speziale, The Weyl BMS group and Einstein's equations, J. High Energy Phys. 07 (2021) 170.
[22] L. Freidel and D. Pranzetti, Gravity from symmetry: Duality and impulsive waves, J. High Energy Phys. 04 (2022) 125.
[23] H. Godazgar, M. Godazgar, and C. N. Pope, New dual gravitational charges, Phys. Rev. D **99**, 024013 (2019).
[24] H. Godazgar, M. Godazgar, and C. N. Pope, Tower of subleading dual BMS charges, J. High Energy Phys. 03 (2019) 057.
[25] U. Kol and M. Porrati, Properties of dual supertranslation charges in asymptotically flat spacetimes, Phys. Rev. D **100**, 046019 (2019).
[26] H. Godazgar, M. Godazgar, and C. N. Pope, Dual gravitational charges and soft theorems, J. High Energy Phys. 10 (2019) 123.
[27] H. Godazgar, M. Godazgar, and M. J. Perry, Asymptotic Gravitational Charges, Phys. Rev. Lett. **125**, 101301 (2020).
[28] H. Godazgar, M. Godazgar, and M. J. Perry, Hamiltonian derivation of dual gravitational charges, J. High Energy Phys. 09 (2020) 084.
[29] R. Oliveri and S. Speziale, A note on dual gravitational charges, J. High Energy Phys. 12 (2020) 079.
[30] U. Kol and M. Porrati, Gravitational Wu-Yang monopoles, Phys. Rev. D **101**, 126009 (2020).
[31] M. Campiglia and A. Laddha, Asymptotic symmetries and subleading soft graviton theorem, Phys. Rev. D **90**, 124028 (2014).
[32] G. Compère, A. Fiorucci, and R. Ruzziconi, Superboost transitions, refraction memory and super-Lorentz charge algebra, J. High Energy Phys. 11 (2018) 200; 04 (2020) 172(E).
[33] G. Compère, R. Oliveri, and A. Seraj, The Poincaré and BMS flux-balance laws with application to binary systems, J. High Energy Phys. 10 (2020) 116.
[34] C. W. Misner, K. S. Thorne, and J. A. Wheeler, *Gravitation* (W. H. Freeman, San Francisco, 1973).
[35] A. Seraj and B. Oblak, Gyroscopic gravitational memory, arXiv:2112.04535.
[36] E. E. Flanagan and D. A. Nichols, Conserved charges of the extended Bondi-Metzner-Sachs algebra, Phys. Rev. D **95**, 044002 (2017).
[37] A. M. Grant and D. A. Nichols, Persistent gravitational wave observables: Curve deviation in asymptotically flat spacetimes, Phys. Rev. D **105**, 024056 (2022).
[38] A. Ashtekar and M. Streubel, Symplectic geometry of radiative modes and conserved quantities at null infinity, Proc. R. Soc. A **376**, 585 (1981).
[39] D. A. Nichols, Spin memory effect for compact binaries in the post-Newtonian approximation, Phys. Rev. D **95**, 084048 (2017).
[40] D. A. Nichols, Center-of-mass angular momentum and memory effect in asymptotically flat spacetimes, Phys. Rev. D **98**, 064032 (2018).
[41] A. Seraj, Gravitational breathing memory and dual symmetries, J. High Energy Phys. 05 (2021) 283.